Water Research 222 (2022) 118916

Contents lists available at ScienceDirect

Water Research

journal homepage: www.elsevier.com/locate/watres

Drivers of spatial and seasonal variations of CO_2 and CH_4 fluxes at the sediment water interface in a shallow eutrophic lake

Heyang Sun [a], Ruihong Yu [a,b,*], Xinyu Liu [a], Zhengxu Cao [a], Xiangwei Li [a], Zhuangzhuang Zhang [a], Jun Wang [a], Shuai Zhuang [a], Zheng Ge [a], Linxiang Zhang [a], Liangqi Sun [a], Andreas Lorke [c], Jie Yang [a,d], Changwei Lu [a], Xixi Lu [a,e,*]

[a] Inner Mongolia Key Laboratory of River and Lake Ecology, School of Ecology and Environment, Inner Mongolia University, Hohhot 010021, China
[b] Key Laboratory of Mongolian Plateau Ecology and Resource Utilization, Ministry of Education, Hohhot 010021, China
[c] Institute for Environmental Sciences, University of Koblenz-Landau, Landau, Germany
[d] Department of Ecology and Environment of Inner Mongolia Autonomous Region, Hohhot 010021, China
[e] Department of Geography, National University of Singapore, 117570, Singapore

ARTICLE INFO

Keywords:
Eutrophication
Lake Ulansuhai
Sediment-water interface
Greenhouse gases
Diffusive fluxes

ABSTRACT

Shallow eutrophic lakes contribute disproportional to the emissions of CO_2 and CH_4 from inland waters. The processes that contribute to these fluxes, their environmental controls, and anthropogenic influences, however, are poorly constrained. Here, we studied the spatial variability and seasonal dynamics of CO_2 and CH_4 fluxes across the sediment-water interface, and their relationships to porewater nutrient concentrations in Lake Ulansuhai, a shallow eutrophic lake located in a semi-arid region in Northern China. The mean concentrations of CO_2 and CH_4 in porewater were 877.8 ± 31.0 μmol L^{-1} and 689.2 ± 45.0 μmol L^{-1}, which were more than 50 and 20 times higher than those in the water column, respectively. The sediment was always a source of both gases for the water column. Porewater CO_2 and CH_4 concentrations and diffusive fluxes across the sediment-water interface showed significant temporal and spatial variations with mean diffusive fluxes of 887.3 ±124.7 μmol m^{-2} d^{-1} and 607.1 ± 68.0 μmol m^{-2} d^{-1} for CO_2 and CH_4, respectively. The temporal and spatial variations of CO_2 and CH_4 concentrations in porewater were associated with corresponding variations in dissolved organic carbon and dissolved nitrogen species. Temperature and dissolved organic carbon in surface porewater were the most important drivers of temporal variations in diffusive fluxes, whereas dissolved organic carbon and nitrogen were the main drivers of their spatial variations. Diffusive fluxes generally increased with increasing dissolved organic carbon and nitrogen in the porewater from the inflow to the outflow region of the lake. The estimated fluxes of both gases at the sediment-water interface were one order of magnitude lower than the emissions at the water surface, which were measured in a companion study. This indicates that diffusive fluxes across the sediment-water interface were not the main pathway for CO_2 and CH_4 emissions to the atmosphere. To improve the mechanistic understanding and predictability of greenhouse gas emissions from shallow lakes, future studies should aim to close the apparent gap in the CO_2 and CH_4 budget by combining improved flux measurement techniques with process-based modeling.

1. Introduction

Carbon dioxide (CO_2) and methane (CH_4) are the two most important greenhouse gases with the increase in their atmospheric concentrations accounting for nearly 80% of the current radiative forcing (Myhre et al., 2014). In relation to their relatively small areal extent, inland waters contribute disproportionately to CO_2 and CH_4 emissions (Downing, 2010; Rosentreter et al., 2021). Yet, current estimates of CO_2 and CH_4 emissions from aquatic ecosystems are not well constrained due to reasons that include the limited number of observations and uncertainties of field measurement (Davidson et al., 2015b; Holgerson and Raymond, 2016; Rosentreter et al., 2021). Quantification of greenhouse gas emissions from various aquatic ecosystems and improved understanding of their environmental drivers are key to improving the

* Corresponding authors.
E-mail address: rhyu@imu.edu.cn (R. Yu).

https://doi.org/10.1016/j.watres.2022.118916
Received 31 December 2021; Received in revised form 25 July 2022; Accepted 27 July 2022
Available online 28 July 2022

accuracy of current CO_2 and CH_4 budgets and their response to climate change and human activities.

Lakes are a vital component of the inland water system regarding carbon cycling and climate regulation, because they store, transport, and transform large quantities of carbon (Tranvik et al., 2009b). Shallow lakes cover the largest surface area globally (Downing et al., 2006; Verpoorter et al., 2014), and are hot spots of CO_2 and CH_4 emissions. It has been demonstrated that sediments in shallow water are particularly important because the CH_4 produced is much more likely to reach the atmosphere, than CH_4 produced in deeper, profundal sediments (Bastviken et al., 2008). Shallow lakes are more vulnerable to eutrophication due to high nutrient input (Anderson et al., 2014; Sinha et al., 2017), and poor self-cleaning capacity (Havens et al., 2001; Sun et al., 2021). Eutrophication plays a critical role in regulating lake CO_2 and CH_4 emissions (Davidson et al., 2015a; Sun et al., 2021).

Lake sediments are the primary site for biogeochemical transformation and can act as a sink or a source of nutrients for the overlying water; therefore, sediments influence the availability of nutrients in lakes (Huang et al., 2017). Both CO_2 and CH_4 can be produced in lake sediments during the microbial degradation of organic carbon by microorganisms (Schimel and Gulledge, 1998; Wang et al., 2017) and is affected by the quantity and quality of organic matter (OM). Eutrophication results in higher OM deposition rates (Hayes et al., 2017), which can cause an increase in carbon burial rates (Heathcote and Downing, 2012; Knoll et al., 2014), or serve as a substrate supporting microbial activity, with the potential to increase CO_2 and CH_4 production (Berberich et al., 2020). Sediment temperature, extent of anoxia, pH, and substrate quantity and quality affect the methanogenesis rate in lake sediments (West et al., 2015). Shallow lakes are inherently heterogeneous over spatiotemporal scales due to changes in topographic features and environmental conditions, resulting in large uncertainties in assessments of their CO_2 and CH_4 budgets and emissions. Although being an important component of basin-scale carbon budgets, spatial and temporal variations of CO_2 and CH_4 concentrations in sediment porewater and fluxes at the sediment-water interface have rarely been studied. Moreover, the linkages between spatio-temporal variability of organic carbon and nutrient availability and sediment – water fluxes have not been studied in shallow eutrophic lakes. Knowledge about the variability and dynamics of diffusive CO_2 and CH_4 fluxes at the sediment-water interface of eutrophic lakes and their main environmental drivers, provides important insights into the lake carbon dynamics and improves the accuracy of carbon and greenhouse gas budgets.

Here we test the hypothesis that porewater CO_2 and CH_4 concentrations and sediment – waters fluxes in shallow eutrophic lakes are characterized by large spatial and seasonal variability in response to temperature and nutrient availability. Using field measurements in an arid, eutrophic, and shallow lake, we evaluated the spatial and seasonal variations of CO_2 and CH_4 porewater concentrations and diffusive fluxes across the sediment-water interface, and identified the main influencing factors of their within-lake variability.

2. Materials and methods

2.1. Study area and sampling sites

Lake Ulansuhai (sometimes translated as Lake Wuliangsuhai) is the largest freshwater lake in the Yellow River basin located in the arid region of the Inner Mongolia Autonomous Region, China (Liu et al., 2017). It is a typical oxbow lake with a surface area of 293 km^2 and a water volume of 2.5-3 $\times$ 10^8 m^3 (Fig. 1). Lake Ulansuhai is the main receiving water body for local agricultural wastewater, domestic sewage, and industrial wastewater, resulting in severe eutrophication. The trophic level in the water column of Lake Ulansuhai is characterized by large spatial heterogeneity and temporal dynamics (Sun et al., 2021). The sampling sites were selected to cover the primary lake areas. Site S1 is located in the northern part of the lake adjacent to the main water inlet, whereas sites S2–S4 are located in the upstream and middle stream regions of the lake. Sites S5 and S6 are close to each other, but the trophic level at site S5 was found to be higher than that at site S6. Site S7 is located near an aquafarm and the outlet of the lake. The highest trophic state occurred at S1, and the lowest occurred at S2 among seven sites (Sun et al., 2021).

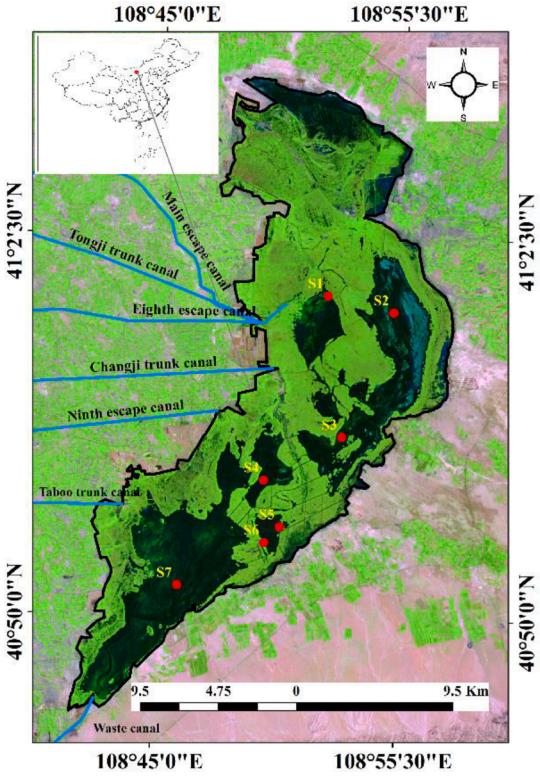

Fig. 1. Map showing the geographic location of Lake Ulansuhai and the locations of the sampling sites (the red points represent sampling points S1-S7). Blue lines show inflow canals and the black line delineates the lake shore. Green areas within the lake indicate emergent aquatic vegetation, while dark green color indicates open water areas. (For interpretation of the references to colour in this figure legend, the reader is referred to the web version of this article.)

2.2. Experimental methods

2.2.1. CO_2 and CH_4 concentrations in water column

Sampling campaigns were conducted in January, May, July, and October in the year 2020. The lake was covered by ice during the campaign in January. During each sampling campaign, the water temperature, pH, and dissolved oxygen concentration (DO) were measured at different water depths using a Multi 3420 analyser (WTW GmbH, Weilheim, Germany) with accuracies of $\pm$ 0.2 °C, $\pm$0.004, and $\pm$ 1.5%, respectively. The concentrations of CO_2 and CH_4 in the water column were measured and calculated using the headspace equilibrium method (Roland et al., 2010). 300 mL of ambient air was sampled 1 m above the lake surface and equilibrated with 800 mL of lake water, which was collected throughout the water column at 0.25 m depth increments using a 2-L organic glass hydrophore (HT-800, Haiter, China). Additional sample was collected at 0.10 m above the sediment. To ensure equilibration, the sample bottle with the headspace was vigorously shaken for 3 min. The equilibrated air was then injected into a pre-vacuumed sampling bag made of gastight aluminum foil and analyzed in a lab using gas chromatography (Shimadzu gas chromatograph GC2030, Kyoto, Japan, equipped with an electron capture

detector (ECD) and flame ionization detector (FID)). The dissolved CO_2 and CH_4 concentrations in the sample C_W were calculated using the following Eq. (1) (Hu et al., 2020; Yang et al., 2019a):

$$C_w = [(C_T - C_A) \times V_T + \alpha \times C_T \times V_W]/V_W \quad (1)$$

Where C_T is the CH_4 or CO_2 concentration (μmol·L^{-1}) in the bottle headspace; C_A is the corresponding atmospheric concentration (μmol·L^{-1}) at the sampling site; V_T is the volume of headspace gas (L) and V_W is the volume of water (L) in the sampling bottle. The temperature dependent Bunsen coefficient α of both gases was calculated according to (Wanninkhof, 1992).

2.2.2. Collection and analysis of porewater samples

Sediment cores were collected from the sampling sites using a gravity sediment corer (tube length 60 cm and inner diameter 9 cm). In total, 28 cores were collected from the 7 sampling areas. To minimize systematic sampling bias, various sites in each sampling area were sampled on each sampling day. The cores were cut to a length of 35 cm, sealed at the top and bottom with silicone plugs, and stored and transported vertically for analysis in the laboratory. From the four cores collected at each point, three cores were used as replicates to determine the dissolved gas concentration and physicochemical variables in pore water. The fourth core was used for the determination of sediment porosity (in triplicates). Porosity (φ) was calculated based on the water content of the sediment, which was determined by weight loss after drying at 105°C for 24 h (Zhang et al., 2013).

In the laboratory, the sediment porewater was extracted from 5, 10, 15, 20, 25, 30 cm depth below the sediment-water interface. The porewater was extracted through drilled holes in the core side wall holes using rhizon tubes (pore size of 0.15 μm, Rhizosphere Research Products B.V., Netherlands) connected to pre-evacuated vials (40 ml volume). This approach causes minimal cross sampling of different sediment layers (Alberto et al., 2000; Bodmer et al., 2020). 20 mL of the extracted porewater was removed using a syringe with a three-way valve and replaced by a headspace filled with air. The samples were shaken vigorously for 1 min to equilibrate porewater and headspace gases before measuring the partial pressures of CO_2 and CH_4 in the headspace using a gas chromatograph (Shimadzu gas chromatograph GC2030, Kyoto, Japan). The porewater concentrations of CO_2 and CH_4 were calculated using Eq. (1) as described above.

The pH value was measured in a porewater aliquot using a Multi 3420 analyser (WTW GmbH, Weilheim, Germany). A 5 mL porewater aliquot was diluted two times and stored frozen prior to analysis of dissolved organic carbon and dissolved total nitrogen (DOC and DTN in mg L^{-1}) using a total organic carbon analyser (Elementar Analyse System GmbH, Langenselbold, Germany) and a multi-N/C analyzer. Each 2 mL porewater aliquot was diluted five times for spectrophotometric measurements (Shimadzu, UV-2600 PC) of the concentrations of ammonium (NH_4^+), nitrite (NO_2^-), nitrate (NO_3^-), and dissolved total phosphorous (DTP).

The diffusive CO_2 and CH_4 flux across the sediment-water interface (SWI) ($F_{S\text{-}W}$, μmol m^{-2} d^{-1}) was calculated using Fick's first law (Boudreau, 1997; Donis et al., 2017; Lerman, 1979; Zhang et al., 2021):

$$F_{S-W} = -\varphi \frac{D_s}{\theta^2} \frac{dc}{dz} \quad (2)$$

where φ is the sediment porosity, θ^2 the tortuosity correction (we used $\theta^2 = 1 - \ln(\varphi)$, (Boudreau, 1997)); D_s (m^2 s^{-1}) the temperature dependent diffusion coefficient of CO_2 and CH_4 in water (Broecker and Peng, 1974) and $\frac{dc}{dz}$ (mmol m^{-4}) is the vertical gradient of dissolved gas concentration below the SWI. For the calculation of the gradient of dissolved CO_2 and CH_4 at the SWI, we considered the gas concentration in overlying water (measured at 10 cm above surface sediment depth) as being representative for the concentration at the SWI and included the first two sampling depths in the sediment. The gradient was determined by linear regression and estimated local diffusive fluxes at the SWI are summarized in Supporting Information Figure S1 and Figure S2. Our approach for estimating fluxes (Eq. (2)) is based on the assumption of steady-state diffusive transport in porewater and is neglecting the effects of gas production and consumption, as well as the possible effect of the water-side concentration boundary layer (Lorke et al., 2003).

2.3. Data analysis

All statistical analyses were performed using SPSS for Windows version 18.0 (SPSS Inc., Chicago, USA). Three-way analyses of variance (ANOVA) were conducted to analyse the influence of sampling month, sampling site, and depth on the concentrations of nutrients and dissolved CO_2 and CH_4 in porewater. Two-way ANOVA were conducted to analyse the influences of sampling month and sampling site on the diffusive fluxes of CO_2 and CH_4. Tukey's post hoc tests were used to identify significant differences ($p<0.05$) between months, sites, and depths. Principal component analysis (PCA) was performed to analyse relationships among the CO_2 and CH_4 concentrations and porewater environmental parameters. Furthermore, a stepwise regression analysis was used to determine the major influential factors for the variability of CO_2 and CH_4 diffusive fluxes across the SWI. The threshold for statistical significance was set to $p<0.05$. Unless otherwise stated, the results are presented as mean value ± standard deviation.

3. Results

3.1. Temporal and spatial variations of nutrients in porewater

Porewater nutrient concentrations (DOC, DTN, DTP, NH_4^+, NO_3^- and NO_2^-) differed significantly between seasons (Fig. 2) and among the seven sites (Fig. S4), whereas the concentrations were similar between different depths below the SWI (the ANOVA results are presented in Table S1 and S2). The concentrations of DOC were lowest in January and slightly higher during the remaining sampling campaigns. In addition, DTN was also lowest in January, but showed more pronounced seasonal variations, with about twofold higher concentrations in July. The majority of DTN was in the form of NH_4^+, which however was less variable in comparison to NO_3^- and NO_2^-. There was no significant difference in DTP concentrations measured in different months.

In addition to seasonal variations, the porewater chemical variables showed some systematic differences among the seven sampling sites (Fig. S4, Table S1 and S2). Most pronounced, sixfold higher DTP concentrations in deeper sediments were observed near the main inflow (S1). Porewater DOC concentrations were highest in the midstream area (S4-S6), where DTN was lowest. The highest and lowest concentrations of DTN and NH_4^+ which were measured near the aquafarm (S7) and site S4, respectively. Sediment porosity was consistently lower in the inflow region (S1) than at the other sites, where it showed similarly low variability among sites and between seasons (Fig. S3).

3.2. Water quality parameters in the water column

Water temperature, pH, and DO in the water column varied significantly among seasons ($p<0.05$) (Fig. 3, Table S3). pH was lowest in January (8.1 ± 0.1) and highest in October (8.9 ± 0.1). Water temperature ranged from -0.3 to 29.7 °C, lowest in winter and highest in summer. DO was highest in October and lowest in July with mean values of 6.9 ± 0.3 and 11.6 ± 0.3 mg L^{-1}, respectively. Spatially, pH varied significantly among different sites ($p<0.05$, Table S3), with the highest and lowest pH values at sites S2 and S4, respectively. The average pH at S4 was nearly one pH unit higher (9.0 ± 0.1) than at S2 (8.2 ± 0.1). Water temperature and DO, in contrast, did not show significant differences between sites. Generally, there were no significant variations in the three variables with water depth (Fig. 3, Table S3), indicating frequent vertical mixing of the water column.

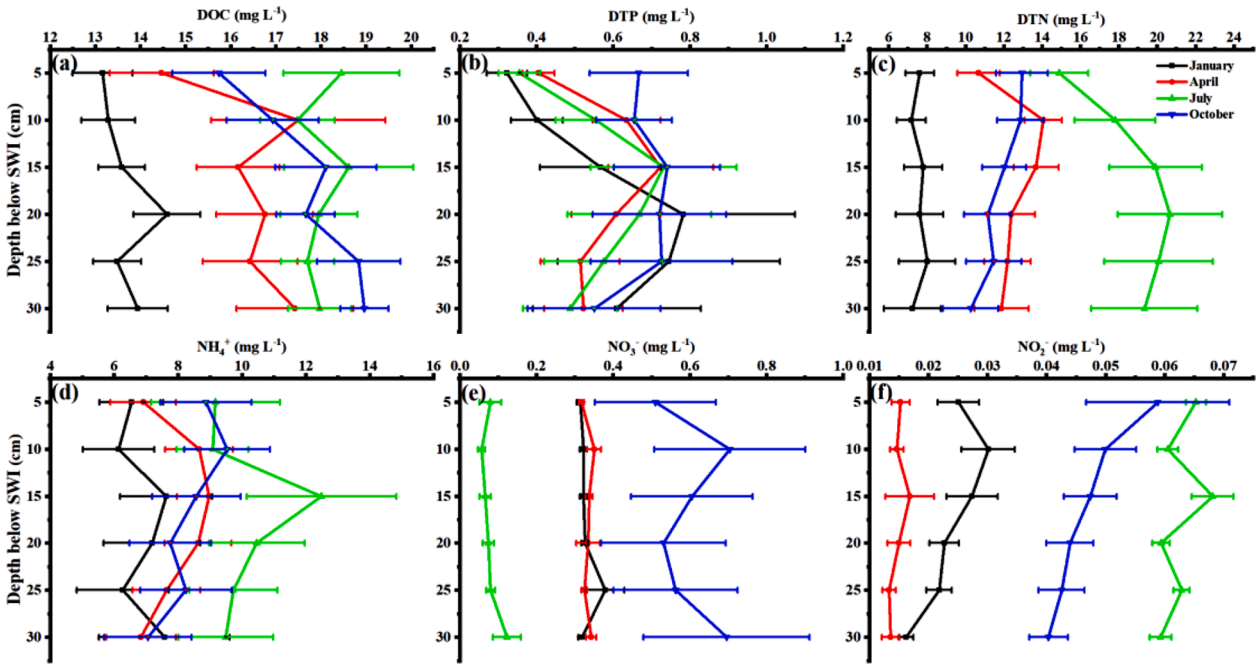

Fig. 2. Temporal variations of water quality variables in sediment porewater. The panels (a) – (f) show the concentrations of DOC, DTP, DTN, NH_4^+, NO_3^- and NO_2^- measured at different depth below the sediment water interface (SWI) during four seasonal sampling campaigns (indicated by different color). Symbols show mean values of the measurements conducted at different sampling sites and error bars show their standard deviation (n = 21).

3.3. Temporal and spatial variations of dissolved CO_2 and CH_4 concentrations

The dissolved CO_2 concentrations in Lake Ulansuhai varied over three orders of magnitude from 16.3 to 4905.0 μmol L^{-1} (Fig. 4a and 4c; the results of the ANOVA are presented in Table S4 and S5). Generally, the vertical profiles showed a steep increase in dissolved CO_2 concentration across SWI, with the mean concentration in porewater (877.8 ± 31.0 μmol L^{-1}) being substantially higher than that in the water column (39.4 ± 1.8 μmol L^{-1}). Overall, the dissolved CO_2 concentrations were higher than atmospheric equilibrium concentrations, except for July, when the water column at site S2 was undersaturated in CO_2 (39.7% saturation). The CO_2 concentrations measured in January were quite different from the other months by being exceptionally low in the porewater, and higher in the water column than in the porewater (Fig. 4a).

In the water column, CO_2 concentrations were highest in July (50.7 ± 2.9 μmol L^{-1}) and lowest in October (28.2 ±0.3 μmol L^{-1}). Spatially, the highest and lowest water-column concentrations were observed at site S5 (46.9 ± 2.9 μmol L^{-1}) and S2 (26.7 ± 1.2 μmol L^{-1}). No significant differences in CO_2 concentrations were observed among different sampling depths.

The porewater CO_2 concentrations varied significantly between months (Fig. 4a), among sites (Fig. 4c), and generally increased with increasing depth below the SWI (Fig. S5a, the results of the ANOVA are presented in Table S6 and S7). The mean porewater CO_2 concentrations were highest in July (2006.1 ± 144.8 μmol L^{-1}) and lowest in January (24.8 ± 0.4 μmol L^{-1}). Spatially, the mean porewater CO_2 concentrations at S5 and S6 (1448.4 ±156.6 μmol L^{-1}) were higher than those observed at other sites, and about threefold higher than the lowest concentrations, which were observed at S1 (462.7 ± 46.0 μmol L^{-1}). From site S2 to S5, porewater CO_2 concentration gradually increased, although not all sites were significantly different from others (Fig. 4c and Table S7). In all measurements, the porewater CO_2 concentrations gradually increased with increasing depth below the SWI with significantly different concentrations at all sampling depths.

Dissolved CH_4 concentrations in the water column varied temporarily over one order of magnitude with the highest concentration in July (17.8 ± 3.0 μmol L^{-1}) and the lowest in April (1.8 ± 0.4 μmol L^{-1}) Fig. 4b). In April and in October, when the concentrations were low, dissolved CH_4 concentrations were similar at all depth, while the concentrations increased towards the water surface in July and had a near-bottom maximum in January (Fig. 4b). The seasonally averaged CH_4 water column concentration was highest at site S3 and lowest at S1, but there were no significant differences among the other sampling sites (S4 to S7, Fig. 4d).

Porewater CH_4 concentrations were approximately 15 times higher than in the water column (Fig. 4b and 4d) and varied over five orders of magnitude from 0.16 to 2297.1 μmol L^{-1}, with an overall mean value of 689.2 ± 45.0 μmol L^{-1}. Similar to CO_2, CH_4 concentrations in the porewater generally increased with increasing depth below the SWI with significant differences between sampling depths ($p<0.01$, Fig. S5b and Table S7). The porewater CH_4 concentrations also showed significant temporal and spatial variations among the four months and seven sites ($p<0.01$), as well as at different sampling depths (Fig. 4b and d and Fig. S5b) (the results of the ANOVA are presented in Table S6 and S7). Temporally, the porewater CH_4 concentrations showed strong seasonal variations among the four sampling months ($p<0.01$), with the lowest value in January (76.4 ± 10.6 μmol L^{-1}), and the highest value in July (1222.9 ±53.2 μmol L^{-1}). Spatially, the mean porewater CH_4 concentrations was highest near the aquafarm (site S7, 952.9 ± 79.9 μmol L^{-1}) and lowest at site S4 (371.3 ± 38.8μmol L^{-1}). From sites S3 to S7, the CH_4 concentrations increased gradually from the inflow to the outflow region of the lake. The spatial variations in porewater CH_4 concentrations differed from those in the water column (Fig. 4d). The highest concentrations in water column were observed at S3 (13.3 ± 2.5 μmol L^{-1}), where the porewater concentrations was lowest (371.3 ± 35.6 μmol L^{-1}), whereas the opposite was observed at S2. It is worth noting that the CH_4 concentration in the water column was very small near the main inflow (site S1).

3.4. Fluxes of CO_2 and CH_4 across sediment-water interface

CO_2 fluxes across SWI in Lake Ulansuhai varied from -1.7 to 5209.0

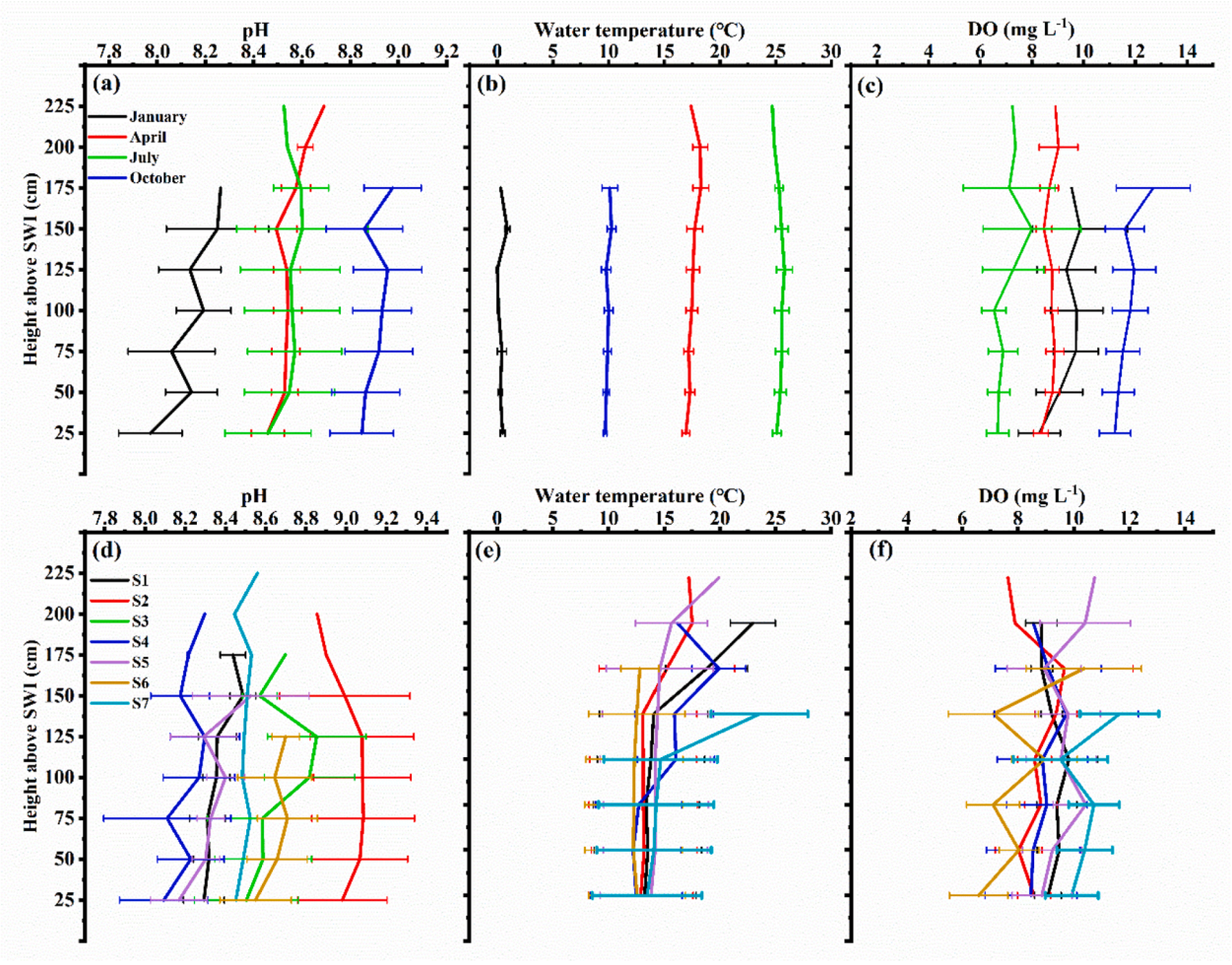

Fig. 3. Temporal and spatial variations of water quality variables in the water column. The panels (a)-(c) show depth profiles of means values of pH, water temperature and DO measured during the seasonal sampling campaigns with error bars showing the standard deviation of measurements taken at seven sampling sites (n=21). (d)-(f) show mean depth profiles observed at the different sampling sites (S1 to S7) with error bars showing the standard deviation of measurements taken at four sampling campaigns (n=12).

μmol m^{-2} d^{-1} (Fig. 5a and 5c), with an overall mean CO_2 flux of 887.3 ± 123.7 μmol m^{-2} d^{-1} (negative fluxes denote CO_2 uptake of the sediment). The fluxes showed remarkable temporal and spatial variations ($p<0.01$) (Table S8 and S9). Temporally, the CO_2 fluxes were largest in July (2241.5 ± 300.3 μmol m^{-2} d^{-1}) and lowest in January (1.7 ± 0.6 μmol m^{-2} d^{-1}). Spatially, the CO_2 fluxes at S6 (1516.4 ± 423.9 μmol m^{-2} d^{-1}) were significantly higher than those at S1, S3, S4 and S7, but similar to S2 and S5. The lowest mean flux was estimated near the inflow at S1 (362.1 ± 110.2 μmol m^{-2} d^{-1}), but was not significantly different from mean fluxes estimated at S3 and near the outlet at S7 (Table S8 and S9).

The diffusive CH_4 fluxes across the SWI ranged from -2.4 to 2271.7 μmol m^{-2} d^{-1}, with a mean value of 607.1 ± 68.0 μmol m^{-2} d^{-1} for the whole sampling period (Fig. 5b and 5d). The CH_4 fluxes showed distinct temporal variations ($p<0.01$) (Table S8 and S9), with the lowest flux in January (43.0 ± 10.0 μmol m^{-2} d^{-1}) and the highest flux in July (1337.0 ± 124.2 μmol m^{-2} d^{-1}). In addition, the CH_4 fluxes also showed significant spatial differences, with the lowest at site S3 (306.5 ± 80.1 μmol m^{-2} d^{-1}) and an about threefold higher flux at S7 (920.9 ± 167.4 μmol m^{-2} d^{-1}).

3.5. Effects of environmental variables on porewater concentrations and diffusive fluxes

Dissolved CO_2 and CH_4 concentrations in porewater were positively correlated to each other, and with DOC, DTN, NH_4^+ and NO_2^- concentrations ($p<0.05$), and negatively correlated with pH ($p<0.05$) (Table 1). DTP was negatively correlated with CO_2 concentrations ($p<0.05$), but not correlated with CH_4 concentrations ($p>0.05$). The principal component analysis (PCA) showed that the variations in porewater CO_2 and CH_4 concentrations were primarily related to variations in DOC, NO_2^- and DTN (Fig. 6a).

The dissolved gas concentrations in porewater were positively correlated with the diffusive fluxes ($p<0.05$, Table 2). Moreover, the diffusive fluxes of CO_2 and CH_4 were positively correlated with each other and increased with increasing concentrations of DOC, DTN, NH_4^+, NO_2^- and sediment temperature ($p<0.05$, Table 2, Fig. 6b). Additionally, the CH_4 flux was higher from sediments with higher porosity. To explore the main controlling factors of the estimated fluxes, a stepwise multiple linear regression analysis was used. The results showed that the surface sediment temperature, DOC, NH_4^+ and NO_2^- were the main influencing factors for the CO_2 fluxes ($p<0.001$), whereas the CH_4 fluxes were mainly influenced by sediment surface temperature and DOC ($p<0.001$) (Table 3).

4. Discussion

4.1. Temporal and spatial variability of CO_2 and CH_4 concentrations

In lakes, especially in shallow lakes, the system metabolism mainly

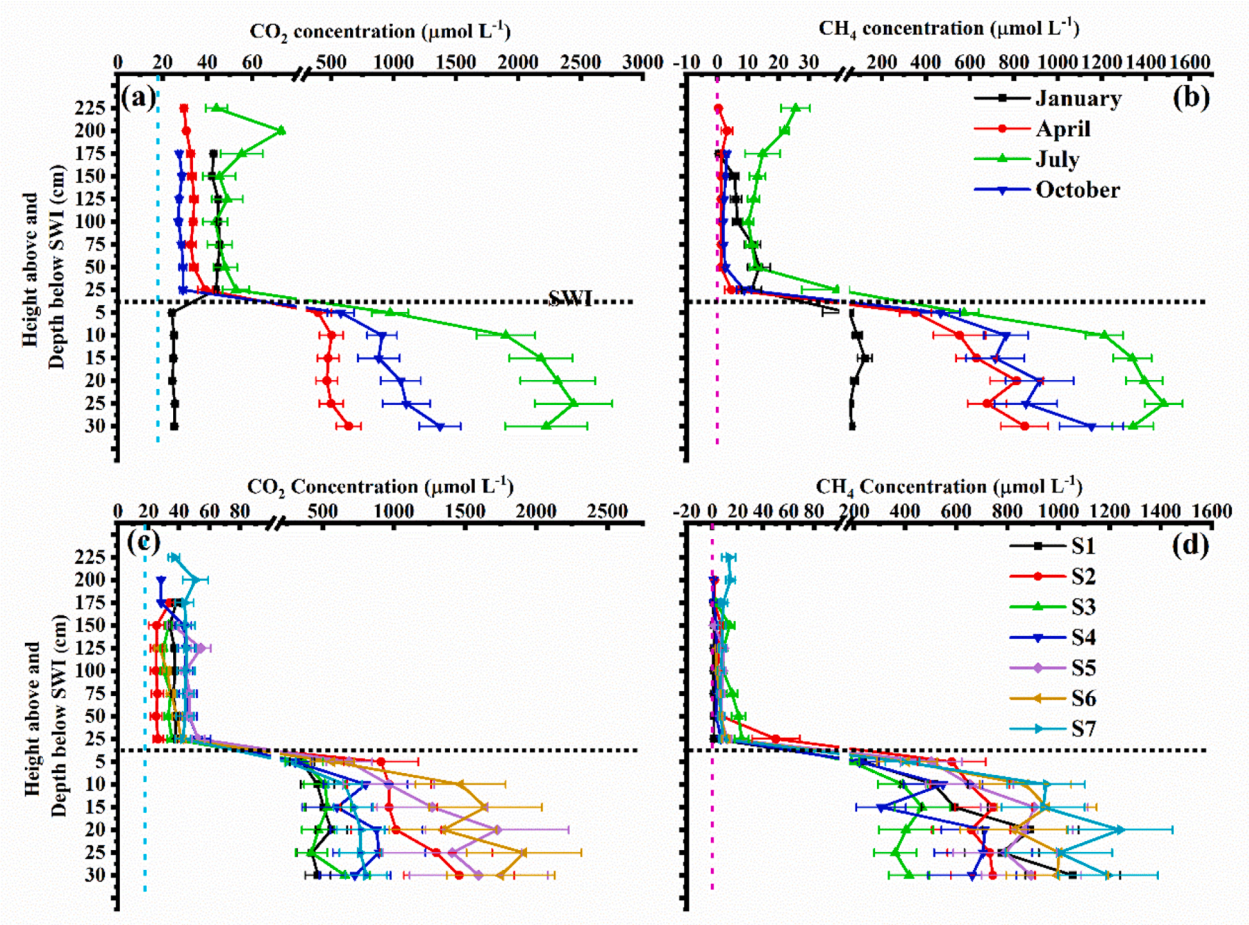

Fig. 4. Staggered concentration profiles of dissolved CO_2 ((a) and (c)) and CH_4 ((b) and (d)) in the water column (measured at different height above the sediment-water interface (SWI) and in porewater (at different depths below the SWI). (a) and (b) show spatially averaged concentration profiles observed during the four seasonal sampling campaigns (error bars show the standard deviation of measurements taken at different sampling sites, n=21). (c) and (d) show the temporarily averaged profiles observed at the different sampling sites (S1 to S7), with error bars showing the standard deviation of four sampling campaigns (n=12). The location of the SWI is indicated by the dashed horizontal line; note the axis break and different axis scaling of the concentration axis at the SWI. The light blue and pink dotted vertical lines indicate the atmospheric equilibrium concentrations of CO_2 and CH_4 (4-month average), respectively. (For interpretation of the references to colour in this figure legend, the reader is referred to the web version of this article.)

occurs in sediments (Bergström et al., 2010). Heterotrophic sediment respiration is the primary source of CO_2 production (Gudasz et al., 2010; MacIntyre et al., 2018; Tranvik et al., 2009a). In this study, measurements in a large, shallow and eutrophic lake revealed large seasonal variations of porewater CO_2 concentrations (Fig. 4a, Table S6), with the mean porewater CO_2 concentrations in July being 80 times higher than in January. The porewater CO_2 concentrations followed a similar temporal dynamic as the concentrations of DOC, DTN, and NO_2^- in the sediment porewater (Fig. 2, and Table 1). The seasonal variations of DOC, DTN, and NO_2^- concentrations explained the majority of the seasonal variations in porewater CO_2 concentrations across all study sites (Fig. 6a). Excess organic carbon (DOC) and nitrogen input potentially provides additional substrate for heterotrophic activity (Kristensen et al., 2008), which causes an increase of the CO_2 concentration in porewater and emission from the sediment to the water. The observed positive effect of NO_2^- on CO_2 concentration may be explained by the production of CO_2 during nitrification and denitrification in the sediment (Hamersley and Howes, 2003). We also found significant spatial variations in porewater CO_2 concentrations, with twofold higher concentration near the lakeshore (S6) compared to the lowest concentration near the inflow (S1, Fig. 4c). The similarity to spatial patterns in nutrient concentration in porewater, and their positive relations with CO_2 concentrations (Table 1 and Fig. 6a), indicate that high nutrient concentrations (DOC, DTN, and NO_2^-) are a crucial determinant for high porewater CO_2 concentration.

Porewater CH_4 concentrations also showed significant temporal and spatial variations in lake Ulansuhai (Fig. 4b and d, Table S6). Temporally, the porewater CH_4 concentrations showed strong seasonal variations, with 15 times higher concentration in summer than in winter. Higher CH_4 production rates at higher temperature (Yvon-Durocher et al., 2014) and increased organic carbon availability from autochthonous production (Fig. 2) are likely promoting the higher CH_4 concentration in summer.

Spatially, we observed persistent gradients with increasing CH_4 concentrations from inlet to the outlet. Relatively higher CH_4 concentrations were found near the lake outlet and the aquafarm (S7), which coincides with higher dissolved nitrogen concentration at this site. It is interesting to note, that this longitudinal gradient is opposing the gradients typically found in deeper lakes and reservoirs, were allochthones organic matter preferably settles near the inflow, leading to higher emissions from these areas (Linkhorst et al., 2021). Indeed, previous studies in Lake Ulansuhai have reported increasing total organic carbon and nutrient content in the sediments from the inflow towards the outflow (Fu et al., 2013; Guo et al., 2014), that results mainly from autochthonous production (Xie et al., 2015).

The spatial pattern observed in Lake Ulansuhai and the results of the correlation analyses suggest that the spatio-temporal variation of porewater CH_4 concentration are mainly driven by different nutrient

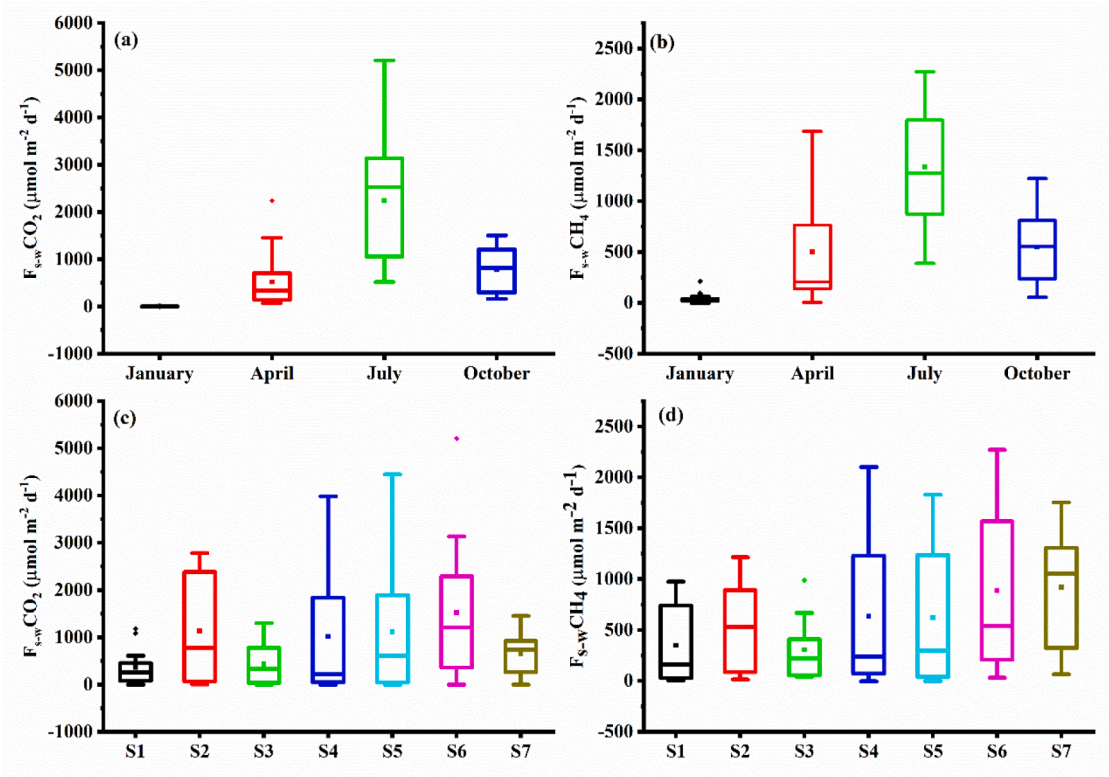

Fig. 5. Temporal and spatial variations of diffusive fluxes of CO_2 and CH_4 across the sediment water interface. The box plots in (a) and (b) show spatial variations estimated from concentration profiles during the four seasonal sampling campaigns. (c) and (d) show temporal variations of flux estimates for the different sampling sites (S1 to S7). Boxes represent the 25th and 75th percentiles, and error bars show the 90th percentiles. The square symbol inside the box, and the horizontal line denote the mean value and the median value, respectively.

Table 1
Pearson correlation coefficients of CO_2 and CH_4 concentrations in porewater with dissolved carbon and nutrient concentrations and pH in the uppermost sediment layer for all sediment cores.

Parameter	CO_2 Concentration	CH_4 Concentration
DOC	0.36**	0.32**
TIN	0.20**	0.38**
DTP	-0.18**	-0.03
NH_4^+	0.13**	0.25**
NO_3^-	-0.05	-0.01
NO_2^-	0.44**	0.35**
pH	-0.16**	-0.17**
CO_2 Concentration	1.00	0.73**
CH_4 Concentration	0.73**	1.00

Note: the * indicates a significant level at 0.05, ** at 0.01; n=504.

concentrations. Moreover, the PCA results further indicated that the spatio-temporal variations of CH_4 concentrations were primarily controlled by the same environmental variables that control porewater CO_2 concentrations (DOC, DTN and NO_2^-, Fig. 6a). Excess nutrients can enhance CH_4 production, leading to the increase of the CH_4 concentrations in porewater (Sepulveda-Jauregui et al., 2018), which were positively correlated with porewater DOC, DTN, and NO_2^- (Table 1). The organic matter content is an important factor facilitating methanogenesis in sediments (Reshmi et al., 2014). Previous studies have shown that the porewater CH_4 concentration is positively influenced by the amount of organic matter, especially its dissolved fraction (Berberich et al., 2020). The mean DOC concentrations in the porewater of Lake Ulansuhai was 16.5 ± 0.2 mg L^{-1}, which can provide sufficient substrate for CH_4 production and in turn increases CH_4 concentrations. In addition, the significant positive effect of DTN on CH_4 concentration is consistent with previous studies (Isidorova et al., 2019). Total nitrogen concentration in sediment can differ and depend on the organic matter source, with N-rich autochthonous organic matter being more biodegradable and produces more CH_4 (Grasset et al., 2018; Meyers, 2003; West et al., 2012). In this study, NO_2^- concentration was an important driver of variations in CH_4 concentrations. NO_2^- is usually considered to be a microbial inhibitor (Tugtas and Pavlostathis, 2007), and it can promote the oxidation of CH_4 at certain concentrations (Nie et al., 2020). However, the results of this study contradict this. One possible explanation for this result is that nitrite can enhance the acidogenic phase resulting in large amounts of low molecular weight organic matter (i.e., acetate), which can be directly utilized by methanogens, resulting in a high methane production rate (Lu et al., 2020).

In addition to quantity, also the quality of organic carbon present in lakes is a key factor controlling CH_4 production under anoxic conditions. The extent to which aquatic vegetation as a source of organic matter leads to the emission of greenhouse gases, or gets buried in the sediment, varies considerably between different vegetation types (Grasset et al., 2018). There are large differences in aquatic plants among the different zones of Lake Ulansuhai, which may be an additional reason for the spatial variations of CH_4 concentrations.

We found that porewater pH had a negative effect on the CO_2 and CH_4 concentrations (Table 1). The accumulation of CO_2 in sediment porewater can alter the carbonate geochemistry resulting in decrease of pH (Taylor et al., 2015). CH_4 is primarily produced by methanogens, which are sensitive to the porewater pH (Chang and Yang, 2003). In Lake Ulansuhai, the pH in surface sediment ranged from 8.0 to 9.4 which may be out of the optimal range for methanogenic archea and partially inhibit their activity (Chang and Yang, 2003; Schrier-Uijl et al., 2011; Yang et al., 2019c).

Furthermore, we found positive correlations between CO_2 and CH_4 concentrations (Table 2). This suggests acetoclastic CH_4 production, where CO_2 is produced in equal molar amounts as CH_4. Interestingly, the

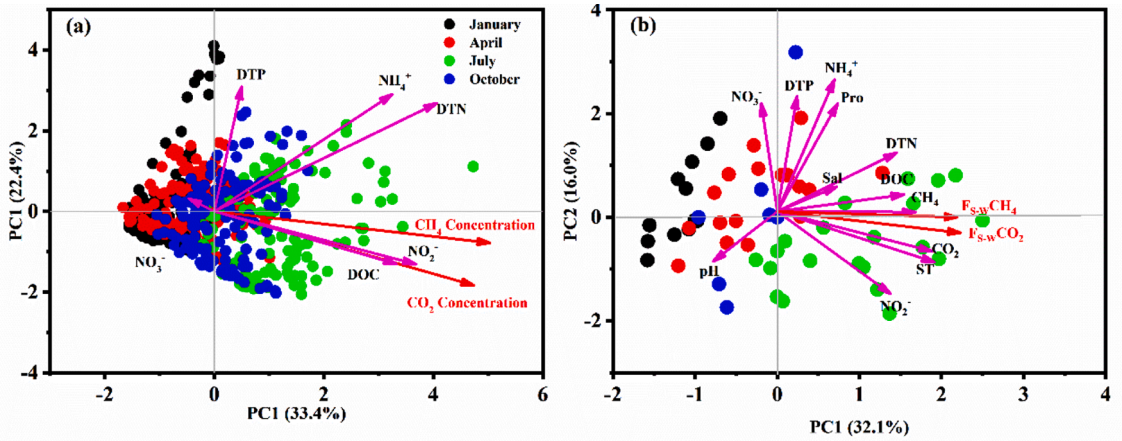

Fig. 6. Principal component analysis bi-plots for the CO_2 (a) and CH_4 (b) concentrations in the porewater, diffusive fluxes of CO_2 (c) and CH_4 (d) across sediment-water interface, and various environmental factors. The graphs show the loadings of environmental factors (arrows) and the scores of observations in different months (symbols with different color).

Table 2
Pearson correlation coefficients of the sediment-water fluxes of CO_2 ($F_{S\text{-}W}CO_2$) and CH_4 ($F_{S\text{-}W}CH_4$) and dissolved carbon and nutrient concentrations, sediment temperature (ST), porosity (Por), pH, and dissolved gas concentration in the uppermost sediment layer of each core.

Parameter	$F_{S\text{-}W}CO_2$	$F_{S\text{-}W}CH_4$
DOC	0.55**	0.42**
DTN	0.48**	0.40**
DTP	0.04	-0.05
NH_4^+	0.40**	0.30**
NO_3^-	-0.12	-0.11
NO_2^-	0.53**	0.48**
ST	0.66**	0.70**
Por	0.19	0.25*
pH	-0.04	0.02
CO_2 Concentration	0.50**	
CH_4 Concentration		0.47**
$F_{S\text{-}W}CO_2$	1.00	0.82**
$F_{S\text{-}W}CH_4$	0.82**	1.00

Note:
* indicates a significant level at 0.05
** at 0.01; n=84.

ratio of CH_4 to CO_2 fluxes at the SWI in Lake Ulansuhai are close to unity ($F_{S\text{-}W}CO_2/F_{S\text{-}W}CH_4$ 108±13%), suggesting that a large share of the sediment C emissions is in the form of CH_4 and that acetoclastic methanogenesis could be the main process for the production of both gases. CH_4 to CO_2 flux ratios smaller than unity indicate contributions of additional aerobic and anaerobic production pathways of CO_2 production. Also anaerobic oxidation of CH_4 can contribute to the production of CO_2 (Ettwig et al., 2008). Denitrification dependent anaerobic methane oxidation can be a major pathway for anaerobic oxidation of CH_4 in freshwater sediments (Raghoebarsing et al., 2006). The occurrence of this oxidation pathway in Lake Ulansuhai is suggested by the positive correlation of CO_2 concentrations with porewater NO_2^- (Table 1).

4.2. Drivers of CO_2 and CH_4 diffusive fluxes

In Lake Ulansuhai, the sediment was a source of CO_2 and CH_4 to the water column. The mean diffusive fluxes of CO_2 (887.3 ± 124.7 μmol m^{-2} d^{-1}) and CH_4 (607.1 ± 68.0 μmol m^{-2} d^{-1}) across the SWI add up to annual CO_2 and CH_4 diffusion emissions of 3.89 and 2.66 g C m^{-2} y^{-1}, respectively. Compared to measurements of surface fluxes reported in our previous study (Sun et al., 2021), which was performed with the same spatial and temporal resolution, the diffusive fluxes across the sediment - water interface account for only $1/40^{th}$ and $1/10^{th}$ of the CO_2 and CH_4 fluxes emitted at to the atmosphere, respectively. This mismatch indicates that the diffusive fluxes across SWI may not be the main source of CO_2 and CH_4 emitted at the water-air interface. Several studies have found that diffusive fluxes at the SWI are not the main pathway for atmospheric emission, with production in the water column and ebullition being the main additional sources of CO_2 and CH_4, respectively (Abe et al., 2005; Gruca-Rokosz et al., 2011). In Lake Ulansuhai, ebullition has been found to be a minor emission pathway, accounting for only 1% of the water-air CH_4 fluxes with a mean value 0.15 mmol m^{-2} d^{-1} (Sun et al., 2021). Alternatively, lateral advection of dissolved CO_2 and CH_4 from zones of enhanced sediment production, such as the vegetated areas or riparian zones, can account for the mismatch between the fluxes across the sediment and air – water interfaces (McGinnis et al., 2016; Sand-Jensen et al., 2019).

Our results were consistent with previous studies, in which significant temporal and spatial variations of diffusive fluxes of CO_2 and CH_4 at the sediment - water interface were found in ponds and lakes (Langenegger et al., 2019; Yang et al., 2019a). Temporally, the diffusive fluxes of CO_2 and CH_4 were of three and two orders of magnitude higher in July compared to January, respectively. The results of stepwise multiple linear regression analysis and PCA between the diffusive fluxes, sediment properties, and nutrient concentrations showed that the surface sediment temperature and concentrations of DOC, NH_4^+ and NO_2^- in porewater were the main controlling factors for variations in CO_2 fluxes, whereas the variations of CH_4 fluxes were mostly related to variations in sediment temperature and DOC (Table 3 and Fig. 6b). Higher

Table 3
Results of stepwise multiple linear regression analysis between diffusive fluxes across the sediment-water interface of CO_2 ($F_{S\text{-}W}CO_2$) and CH_4 ($F_{S\text{-}W}CH_4$) and environmental parameters (ST sediment temperature, DOC dissolved organic carbon, NH_4^+ ammonium concentration, and nitrite concentration) in the surface sediment

Flux	Regression equations	F	R^2	p	N
Fs-wCO_2	Y=64.70ST+52.30DOC+42.21NH_4^++ 10664.47NO_2^--1573.21	25.19	0.639	<0.001	84
Fs-wCH_4	Y=47.96ST+29.83DOC-486.95	32.76	0.526	<0.001	84

temperature stimulates carbon mineralization rates and the production of CO_2 (Gudasz et al., 2010), resulting in higher CO_2 porewater concentrations and higher fluxes from the sediments to the overlying water (Xiong et al., 2017; Yang et al., 2019a) (Table 2, Fig. 6b). Similarly, rates of methanogenesis increase with increasing temperature (Grasset et al., 2018; Sepulveda-Jauregui et al., 2018), which contributes to the seasonal variations of the diffusive fluxes also in Lake Ulansuhai. The CO_2 and CH_4 fluxes were both influenced by DOC (Tables 2 and 3, Fig. 6b), which demonstrates that excess carbon availability in the sediment promotes higher CO_2 and CH_4 fluxes, and supports findings from previous studies (Sobek et al., 2012; Xiong et al., 2017; Yang et al., 2019b). The spatial variations of the CO_2 and CH_4 fluxes were relatively small in comparison to the temporal variations. Similar spatial variations were observed in the CO_2 and CH_4 fluxes and in porewater concentrations, which indicates that spatial variations in local CO_2 and CH_4 production rates were the main cause for the observed differences in sediment – water fluxes. The spatial variations in production rates were related to variations in dissolved organic carbon and nitrogen concentrations in the porewater of surface sediment, which, besides temperature, were the main controlling factors for CO_2 and CH_4 fluxes (Table 3 and Fig. 6b). The trophic status of the water and the sediment has been previously reported as an important factor regulating CH_4 emissions at the basin scale (Beaulieu et al., 2019; Schrier-Uijl et al., 2011; Sepulveda-Jauregui et al., 2018). Our results demonstrate, that spatial variations in the availability of organic carbon and nitrogen in the sediment porewater can results in large variability of CO_2 and CH_4 fluxes within individual aquatic ecosystems.

4.3. Limitation and future research

The large spatial and temporal variability of dissolved gas concentrations and fluxes at the SWI observed in our measurements, demonstrate that robust basin-scale estimates of carbon cycling and greenhouse gas emissions in Lake Ulansuhai would require more sampling sites and higher frequency sampling. While such measurements became feasible for resolving the spatial variations in surface water concentrations and diffusive emissions at the air-water interface (Liu et al., 2021; Xiao et al., 2020), no appropriate method exists for mapping porewater concentrations and sediment-water fluxes. Moreover, our results rely on indirect estimates of the fluxes from measured porewater concentration profiles. For the calculation of sediment-water fluxes, we assumed steady-state diffusive transport in porewater and neglected the effects of gas production and consumption. Moreover, the concentration at the SWI had to be approximated by the concentration measured in the overlying water, thereby neglecting the influence of the concentration boundary layer above the SWI. The existence of a water-side concentration boundary layer would cause a lower concentration at the SWI and lower fluxes. Our flux estimates can therefore be considered as upper bounds.

The flux estimates can be improved by direct measurements under in situ conditions. Such measurements could be obtained by applying the aquatic eddy correlation technique (Donis et al., 2015), which, however requires fast-response sensors for concentration measurements and has been nearly exclusively used for measuring oxygen fluxes at the SWI in lakes and rivers. A variant of the eddy-correlation technique, that would allow flux estimates at the SWI for a larger group of compounds, including nutrients, and dissolved CO_2 and CH_4 concentrations, has been proposed recently (Lemaire et al., 2017), but not yet successfully implemented in aquatic research. Besides in-situ measurements, flux estimates can be improved by estimating production rates in different sediment layers in ex situ incubations in future studies. These rates can be used to extent the diffusive transport model (Equation 2) to include reactions (Sabrekov et al., 2017; Tang et al., 2010), and eventually become integrated in larger-scale models that can additionally assist in upscaling the findings to the basin scale.

5. Conclusions

In this study, we investigated the diffusive fluxes of CO_2 and CH_4 across the SWI in relation to nutrient concentrations in the shallow eutrophic Lake Ulansuhai at different seasons. The study explored the dynamics of CO_2 and CH_4 in a hypereutrophic lake sediment, demonstrating large spatial and temporal variations in concentrations and diffusive fluxes of both greenhouse gases in the porewater and at the SWI. The sediment was a source of CO_2 and CH_4 to the water column, yet, the diffusive fluxes of CO_2 and CH_4 at the SWI were one order of magnitude smaller than the corresponding fluxes at the water-air interface, showing that the diffusive fluxes were not the major emission pathway of CO_2 and CH_4 to atmosphere. Seasonal variations in surface sediment temperature were an important driver of temporal changes in CO_2 and CH_4 fluxes at the SWI. In addition, we found that higher organic carbon and nitrogen concentrations in the sediment porewater were associated with higher CO_2 and CH_4 concentrations and promoted higher CO_2 and CH_4 fluxes to the water column. In contrast to deeper lakes and reservoirs, the concentration of organic carbon and nutrients in sediment porewater and the diffusive fluxes of CO_2 and CH_4 at the sediment – water interface increased from the inflow to the outflow region of Lake Ulansuhai. Our results show that the trophic status is an important driver of CO_2 and CH_4 fluxes from sediments and their spatial variations within heterogeneous aquatic ecosystems. We suggest that efforts to reduce excess nutrient input to inland waters should be accelerated to reduce the climatic impact of cultural eutrophication.

CRediT authorship contribution statement

Heyang Sun: Conceptualization, Methodology, Investigation, Formal analysis, Writing – original draft, Writing – review & editing. **Ruihong Yu:** Methodology, Conceptualization, Writing – original draft, Writing – review & editing. **Xinyu Liu:** Conceptualization, Investigation, Methodology. **Zhengxu Cao:** Investigation, Methodology. **Xiangwei Li:** Investigation, Methodology. **Zhuangzhuang Zhang:** Investigation, Methodology. **Jun Wang:** Investigation. **Shuai Zhuang:** Investigation. **Zheng Ge:** Investigation. **Linxiang Zhang:** Investigation. **Liangqi Sun:** Investigation. **Andreas Lorke:** Conceptualization, Methodology, Writing – review & editing. **Jie Yang:** Conceptualization, Writing – original draft, Writing – review & editing. **Changwei Lu:** Conceptualization, Methodology. **Xixi Lu:** Conceptualization, Methodology, Writing – original draft, Writing – review & editing.

Declaration of Competing Interest

The authors declare that they have no known competing financial interests or personal relationships that could have influenced the work reported in this paper.

Data Availability

The authors do not have permission to share data.

Acknowledgments

This study was funded by the National Natural Science Foundation of China (grant no. 51869014), National Key Research and Development Program of China (grant no. 2021YFC3201200), Major Science and Technology Projects of Inner Mongolia Autonomous Region (grant nos. 2020ZD0009 and ZDZX2018054), Key Scientific and Technological Project of Inner Mongolia (grant no. 2019GG019), and Open Project Program of the Ministry of Education Key Laboratory of Ecology and Resources Use of the Mongolian Plateau (grant no. KF2020006).

Supplementary materials

Supplementary material associated with this article can be found, in the online version, at doi:10.1016/j.watres.2022.118916.

References

Abe, D.S., Adams, D.D., Galli, C.V.S., Sikar, E., Tundisi, J.G., 2005. Sediment greenhouse gases (methane and carbon dioxide) in the Lobo-Broa Reservoir, Sao Paulo State, Brazil: Concentrations and diffuse emission fluxes for carbon budget considerations. Lakes & Reservoirs Res. Manage. 10 (4), 201–209.

Alberto, M., Arah, J., Neue, H., Wassmann, R., Lantin, R., Aduna, J., Bronson, K., 2000. A sampling technique for the determination of dissolved methane in soil solution. Chemosphere-Global Change Sci. 2 (1), 57–63.

Anderson, N.J., Bennion, H., Lotter, A.F., 2014. Lake eutrophication and its implications for organic carbon sequestration in Europe. Global Change Biol. 20 (9), 2741–2751.

Bastviken, D., Cole, J.J., Pace, M.L., Van de Bogert, M.C., 2008. Fates of methane from different lake habitats: Connecting whole-lake budgets and CH_4 emissions. J. Geophys. Res.: Biogeosci. 113 (G2).

Beaulieu, J.J., DelSontro, T., Downing, J.A., 2019. Eutrophication will increase methane emissions from lakes and impoundments during the 21st century. Nat. Commun. 10 (1), 1375.

Berberich, M.E., Beaulieu, J.J., Hamilton, T.L., Waldo, S., Buffam, I., 2020. Spatial variability of sediment methane production and methanogen communities within a eutrophic reservoir: Importance of organic matter source and quantity. Limnol. Oceanogr. 65 (6), 1336–1358.

Bergström, I., Kortelainen, P., Sarvala, J., Salonen, K., 2010. Effects of temperature and sediment properties on benthic CO_2 production in an oligotrophic boreal lake. Freshwater Biol. 55 (8), 1747–1757.

Bodmer, P., Wilkinson, J., Lorke, A., 2020. Sediment properties drive spatial variability of potential methane production and oxidation in small streams. J. Geophys. Res.-Biogeosci. 125 (1).

Boudreau, B.P., 1997. Diagenetic models and their implementation. Springer, Berlin.

Broecker, W.S., Peng, T.H., 1974. Gas exchange rates between air and sea. Tellus 26 (1/2), 21–35.

Chang, T.-C., Yang, S.-S., 2003. Methane emission from wetlands in Taiwan. Atmos. Environ. 37 (32), 4551–4558.

Davidson, T.A., Audet, J., Svenning, J.C., Lauridsen, T.L., Sondergaard, M., Landkildehus, F., Larsen, S.E., Jeppesen, E., 2015a. Eutrophication effects on greenhouse gas fluxes from shallow-lake mesocosms override those of climate warming. Glob. Chang. Biol. 21 (12), 4449–4463.

Davidson, T.A., Audet, J., Svenning, J.C., Lauridsen, T.L., Søndergaard, M., Landkildehus, F., Larsen, S.E., Jeppesen, E., 2015b. Eutrophication effects on greenhouse gas fluxes from shallow-lake mesocosms override those of climate warming. Glob. Change Biol. 21 (12), 4449–4463.

Donis, D., Flury, S., Stöckli, A., Spangenberg, J.E., Vachon, D., McGinnis, D.F., 2017. Full-scale evaluation of methane production under oxic conditions in a mesotrophic lake. Nat. Commun. 8 (1), 1–12.

Donis, D., Holtappels, M., Noss, C., Cathalot, C., Hancke, K., Polsenaere, P., Wenzhöfer, F., Lorke, A., Meysman, F.J., Glud, R.N., 2015. An assessment of the precision and confidence of aquatic eddy correlation measurements. J. Atmos. Oceanic Technol. 32 (3), 642–655.

Downing, J.A., 2010. Emerging global role of small lakes and ponds: little things mean a lot. Limnetica 29 (1), 0009–0024.

Downing, J.A., Prairie, Y., Cole, J., Duarte, C., Tranvik, L., Striegl, R.G., McDowell, W., Kortelainen, P., Caraco, N., Melack, J., 2006. The global abundance and size distribution of lakes, ponds, and impoundments. Limnol. Oceanogr. 51 (5), 2388–2397.

Ettwig, K.F., Shima, S., Van De Pas-Schoonen, K.T., Kahnt, J., Medema, M.H., Op Den Camp, H.J., Jetten, M.S., Strous, M., 2008. Denitrifying bacteria anaerobically oxidize methane in the absence of Archaea. Environ. Microbiol. 10 (11), 3164–3173.

Fu, X., Jia, K., Shi, X., Zhao, S., Cui, F., Fan, C., Gao, H., 2013. The humus composition and distribution of Lake Wuliangsuhai sediment. Hupo Kexue 25 (4), 489–496.

Grasset, C., Mendonça, R., Villamor Saucedo, G., Bastviken, D., Roland, F., Sobek, S., 2018. Large but variable methane production in anoxic freshwater sediment upon addition of allochthonous and autochthonous organic matter. Limnol. Oceanogr. 63 (4), 1488–1501.

Gruca-Rokosz, R., Tomaszek, J.A., Koszelnik, P., Czerwieniec, E., 2011. Methane and carbon dioxide fluxes at the sediment-water interface in reservoir. Polish J. Environ. Stud. 20 (1), 81–86.

Gudasz, C., Bastviken, D., Steger, K., Premke, K., Sobek, S., Tranvik, L.J., 2010. Temperature-controlled organic carbon mineralization in lake sediments. Nature 466 (7305), 478–481.

Guo, X.J., He, L.S., Li, Q., Yuan, D.H., Deng, Y., 2014. Investigating the spatial variability of dissolved organic matter quantity and composition in Lake Wuliangsuhai. Ecol. Eng. 62, 93–101.

Hamersley, M.R., Howes, B.L., 2003. Contribution of denitrification to nitrogen, carbon, and oxygen cycling in tidal creek sediments of a New England salt marsh. Marine Ecol. Progress Series 262, 55–69.

Havens, K., Fukushima, T., Xie, P., Iwakuma, T., James, R., Takamura, N., Hanazato, T., Yamamoto, T., 2001. Nutrient dynamics and the eutrophication of shallow lakes Kasumigaura (Japan), Donghu (PR China), and Okeechobee (USA). Environ. Pollut. 111 (2), 263–272.

Hayes, N.M., Deemer, B.R., Corman, J.R., Razavi, N.R., Strock, K.E., 2017. Key differences between lakes and reservoirs modify climate signals: A case for a new conceptual model. Limnol. Oceanography Lett. 2 (2), 47–62.

Heathcote, A.J., Downing, J.A., 2012. Impacts of eutrophication on carbon burial in freshwater lakes in an intensively agricultural landscape. Ecosystems 15 (1), 60–70.

Holgerson, M.A., Raymond, P.A., 2016. Large contribution to inland water CO_2 and CH_4 emissions from very small ponds. Nat. Geosci. 9 (3), 222–226.

Hu, B., Wang, D., Meng, W., Zhou, J., Sun, Z., Liu, X., 2020. Greenhouse gas diffusive fluxes at the sediment–water interface of sewage-draining rivers. J. Soils Sediments 20, 3243–3253.

Huang, W., Chen, X., Jiang, X., Zheng, B., 2017. Characterization of sediment bacterial communities in plain lakes with different trophic statuses. Microbiol. Open 6 (5), e00503.

Isidorova, A., Grasset, C., Mendonça, R., Sobek, S., 2019. Methane formation in tropical reservoirs predicted from sediment age and nitrogen. Sci. Rep. 9 (1), 1–9.

Knoll, L.B., Vanni, M.J., Renwick, W.H., Kollie, S., 2014. Burial rates and stoichiometry of sedimentary carbon, nitrogen and phosphorus in M idwestern US reservoirs. Freshwater Biol. 59 (11), 2342–2353.

Kristensen, E., Bouillon, S., Dittmar, T., Marchand, C., 2008. Organic carbon dynamics in mangrove ecosystems: a review. Aquatic Botany 89 (2), 201–219.

Langenegger, T., Vachon, D., Donis, D., McGinnis, D.F., 2019. What the bubble knows: Lake methane dynamics revealed by sediment gas bubble composition. Limnol. Oceanogr. 64 (4), 1526–1544.

Lemaire, B.J., Noss, C., Lorke, A., 2017. Toward relaxed eddy accumulation measurements of sediment-water exchange in aquatic ecosystems. Geophys. Res. Lett. 44 (17), 8901–8909.

Lerman, A., 1979. Geochemical processes. Water and sediment environments. John Wiley and Sons, Inc.

Linkhorst, A., Paranaiba, J.R., Mendonca, R., Rudberg, D., DelSontro, T., Barros, N., Sobek, S., 2021. Spatially resolved measurements in tropical reservoirs reveal elevated methane ebullition at river inflows and at high productivity. Global Biogeochem. Cycles 35 (5).

Liu, J., Xiao, S., Wang, C., Yang, Z., Liu, D., Guo, X., Liu, L., Lorke, A., 2021. Spatial and temporal variability of dissolved methane concentrations and diffusive emissions in the Three Gorges Reservoir. Water Res. 207, 117788.

Liu, Y., Li, C.Y., Anderson, B., Zhang, S., Shi, X.H., Zhao, S.N., 2017. A modified QWASI model for fate and transport modeling of mercury between the water-ice-sediment in Lake Ulansuhai. Chemosphere 176, 117–124.

Lorke, A., Muller, B., Maerki, M., Wuest, A., 2003. Breathing sediments: The control of diffusive transport across the sediment-water interface by periodic boundary-layer turbulence. Limnol. Oceanogr. 48 (6), 2077–2085.

Lu, Y.Q., Xu, Y., Chen, S.S., Dong, B., Dai, X.H., 2020. Effect of nitrite addition on the two-phase anaerobic digestion of waste activated sludge: Optimization of the acidogenic phase and influence mechanisms. Environ. Pollut. 261.

MacIntyre, S., Cortés, A., Sadro, S., 2018. Sediment respiration drives circulation and production of CO_2 in ice-covered Alaskan arctic lakes. Limnol. Oceanography Lett. 3 (3), 302–310.

McGinnis, D.F., Bilsley, N., Schmidt, M., Fietzek, P., Bodmer, P., Premke, K., Lorke, A., Flury, S., 2016. Deconstructing Methane Emissions from a Small Northern European River: Hydrodynamics and Temperature as Key Drivers. Environ. Sci. Technol. 50 (21), 11680–11687.

Meyers, P.A., 2003. Applications of organic geochemistry to paleolimnological reconstructions: a summary of examples from the Laurentian Great Lakes. Org. Geochem. 34 (2), 261–289.

Myhre, G., Shindell, D., Pongratz, J., 2014. Anthropogenic and natural radiative forcing.

Nie, W.-B., Ding, J., Xie, G.-J., Yang, L., Peng, L., Tan, X., Liu, B.-F., Xing, D.-F., Yuan, Z., Ren, N.-Q., 2020. Anaerobic oxidation of methane coupled with dissimilatory nitrate reduction to ammonium fuels anaerobic ammonium oxidation. Environ. Sci. Technol. 55 (2), 1197–1208.

Raghoebarsing, A.A., Pol, A., Van de Pas-Schoonen, K.T., Smolders, A.J., Ettwig, K.F., Rijpstra, W.I.C., Schouten, S., Damsté, J.S.S., Op den Camp, H.J., Jetten, M.S., 2006. A microbial consortium couples anaerobic methane oxidation to denitrification. Nature 440 (7086), 918–921.

Roland, F., Vidal, L.O., Pacheco, F.S., Barros, N.O., Assireu, A., Ometto, J.P., Cimbleris, A.C., Cole, J.J., 2010. Variability of carbon dioxide flux from tropical (Cerrado) hydroelectric reservoirs. Aquat. Sci. 72 (3), 283–293.

Rosentreter, J.A., Borges, A.V., Deemer, B.R., Holgerson, M.A., Liu, S., Song, C., Melack, J., Raymond, P.A., Duarte, C.M., Allen, G.H., 2021. Half of global methane emissions come from highly variable aquatic ecosystem sources. Nat. Geosci. 14 (4), 225–230.

Sabrekov, A.F., Runkle, B.R.K., Glagolev, M.V., Terentieva, I.E., Stepanenko, V.M., Kotsyurbenko, O.R., Maksyutov, S.S., Pokrovsky, O.S., 2017. Variability in methane emissions from West Siberia's shallow boreal lakes on a regional scale and its environmental controls. Biogeosciences 14 (15), 3715–3742.

Sand-Jensen, K., Andersen, M.R., Martinsen, K.T., Borum, J., Kristensen, E., Kragh, T., 2019. Shallow plant-dominated lakes - extreme environmental variability, carbon cycling and ecological species challenges. Ann. Bot. 124 (3), 355–366.

Schimel, J.P., Gulledge, J., 1998. Microbial community structure and global trace gases. Global Change Biol. 4 (7), 745–758.

Schrier-Uijl, A., Veraart, A., Leffelaar, P., Berendse, F., Veenendaal, E., 2011. Release of CO_2 and CH_4 from lakes and drainage ditches in temperate wetlands. Biogeochemistry 102 (1), 265–279.

Sepulveda-Jauregui, A., Hoyos-Santillan, J., Martinez-Cruz, K., Walter Anthony, K.M., Casper, P., Belmonte-Izquierdo, Y., Thalasso, F., 2018. Eutrophication exacerbates the impact of climate warming on lake methane emission. Sci. Total Environ. 636, 411–419.

Sinha, E., Michalak, A., Balaji, V., 2017. Eutrophication will increase during the 21st century as a result of precipitation changes. Science 357 (6349), 405–408.
Sobek, S., DelSontro, T., Wongfun, N., Wehrli, B., 2012. Extreme organic carbon burial fuels intense methane bubbling in a temperate reservoir. Geophys. Res. Lett. 39 (1).
Sun, H., Lu, X., Yu, R., Yang, J., Liu, X., Cao, Z., Zhang, Z., Li, M., Geng, Y., 2021. Eutrophication decreased CO_2 but increased CH_4 emissions from lake: A case study of a shallow Lake Ulansuhai. Water Res., 117363
Tang, J., Zhuang, Q., Shannon, R.D., White, J.R., 2010. Quantifying wetland methane emissions with process-based models of different complexities. Biogeosciences 7 (11), 3817–3837.
Taylor, P., Lichtschlag, A., Toberman, M., Sayer, M.D., Reynolds, A., Sato, T., Stahl, H., 2015. Impact and recovery of pH in marine sediments subject to a temporary carbon dioxide leak. Int. J. Greenhouse Gas Control 38, 93–101.
Tranvik, L.J., Downing, J.A., Cotner, J.B., Loiselle, S.A., Striegl, R.G., Ballatore, T.J., Dillon, P., Finlay, K., Fortino, K., Knoll, L.B., 2009a. Lakes and reservoirs as regulators of carbon cycling and climate. Limnol. Oceanogr. 54 (6part2), 2298–2314.
Tranvik, L.J., Downing, J.A., Cotner, J.B., Loiselle, S.A., Striegl, R.G., Ballatore, T.J., Dillon, P., Finlay, K., Fortino, K., Knoll, L.B., Kortelainen, P.L., Kutser, T., Larsen, S., Laurion, I., Leech, D.M., McCallister, S.L., McKnight, D.M., Melack, J.M., Overholt, E., Porter, J.A., Prairie, Y., Renwick, W.H., Roland, F., Sherman, B.S., Schindler, D.W., Sobek, S., Tremblay, A., Vanni, M.J., Verschoor, A.M., von Wachenfeldt, E., Weyhenmeyer, G.A., 2009b. Lakes and reservoirs as regulators of carbon cycling and climate. Limnol. Oceanogr. 54 (6), 2298–2314.
Tugtas, A.E., Pavlostathis, S.G., 2007. Inhibitory effects of nitrogen oxides on a mixed methanogenic culture. Biotechnol. Bioeng. 96 (3), 444–455.
Verpoorter, C., Kutser, T., Seekell, D.A., Tranvik, L.J., 2014. A global inventory of lakes based on high-resolution satellite imagery. Geophys. Res. Lett. 41 (18), 6396–6402.
Wang, H., Yu, L., Zhang, Z., Liu, W., Chen, L., Cao, G., Yue, H., Zhou, J., Yang, Y., Tang, Y., 2017. Molecular mechanisms of water table lowering and nitrogen deposition in affecting greenhouse gas emissions from a Tibetan alpine wetland. Global Change Biol. 23 (2), 815–829.
Wanninkhof, R., 1992. Relationship between wind speed and gas exchange over the ocean. J. Geophys. Res.: Oceans 97 (C5), 7373–7382.
West, W.E., Coloso, J.J., Jones, S.E., 2012. Effects of algal and terrestrial carbon on methane production rates and methanogen community structure in a temperate lake sediment. Freshwater Biol. 57 (5), 949–955.
West, W.E., McCarthy, S.M., Jones, S.E., 2015. Phytoplankton lipid content influences freshwater lake methanogenesis. Freshwater Biol. 60 (11), 2261–2269.
Xiao, S., Liu, L., Wang, W., Lorke, A., Woodhouse, J., Grossart, H.-P., 2020. A Fast-Response Automated Gas Equilibrator (FaRAGE) for continuous in situ measurement of CH 4 and CO 2 dissolved in water. Hydrol. Earth Syst. Sci. 24 (7), 3871–3880.
Xie, Z., He, J., Lü, C., Zhang, R., Zhou, B., Mao, H., Song, W., Zhao, W., Hou, D., Wang, J., 2015. Organic carbon fractions and estimation of organic carbon storage in the lake sediments in Inner Mongolia Plateau, China. Environ. Earth Sci. 73 (5), 2169–2178.
Xiong, Y., Wang, F., Guo, X., Liu, F., Dong, S., 2017. Carbon dioxide and methane fluxes across the sediment-water interface in different grass carp Ctenopharyngodon idella polyculture models. Aquac. Environ. Interact. 9, 45–56.
Yang, P., Lai, D.F., Yang, H., Tong, C., 2019a. Carbon dioxide dynamics from sediment, sediment-water interface and overlying water in the aquaculture shrimp ponds in subtropical estuaries, southeast China. J. Environ. Manage. 236, 224–235.
Yang, P., Lai, D.Y., Yang, H., Tong, C., Lebel, L., Huang, J., Xu, J., 2019b. Methane dynamics of aquaculture shrimp ponds in two subtropical estuaries, southeast China: dissolved concentration, net sediment release, and water oxidation. J. Geophys. Res.: Biogeosciences 124 (6), 1430–1445.
Yang, P., Zhang, Y., Yang, H., Zhang, Y., Xu, J., Tan, L., Tong, C., Lai, D.Y., 2019c. Large fine-scale spatiotemporal variations of CH_4 diffusive fluxes from shrimp aquaculture ponds affected by organic matter supply and aeration in Southeast China. J. Geophys. Res.: Biogeosciences 124 (5), 1290–1307.
Yvon-Durocher, G., Allen, A.P., Bastviken, D., Conrad, R., Gudasz, C., St-Pierre, A., Thanh-Duc, N., Del Giorgio, P.A., 2014. Methane fluxes show consistent temperature dependence across microbial to ecosystem scales. Nature 507 (7493), 488–491.
Zhang, L., Liao, Q., Gao, R., Luo, R., Liu, C., Zhong, J., Wang, Z., 2021. Spatial variations in diffusive methane fluxes and the role of eutrophication in a subtropical shallow lake. Sci. Total Environ. 759, 143495.
Zhang, L., Wang, L., Yin, K., Lü, Y., Zhang, D., Yang, Y., Huang, X., 2013. Pore water nutrient characteristics and the fluxes across the sediment in the Pearl River estuary and adjacent waters, China. Estuarine Coastal Shelf Sci. 133, 182–192.